International Journal of Applied Electrical and Electronics Engineering
Volume 2, Issue 2, 2026

Forecasting Solar Irradiance Over Time using Multilinear Predictors

Dan, Micu. Faculty of Electrical Engineering, Technical University of Cluj-Napoca, Cluj-Napoca, Romania

Research Article

Date of Submission: 23-04-2026 Date of Acceptance: 11-05-2026 Date of Publication: 9-06-2026

Abstract—Prices and pollution are rising in tandem with the daily increase in demand for crude oil, which is detrimental to the environment. In order to save the environment and provide humans a better energy source, greater efforts are being made to generate clean energy. New problems and difficulties have surfaced as the renewable energy industry expands. Energy transmission and storage systems have difficulties due to the unpredictability of electricity output from wind turbines, solar power plants, and dams. Machine learning methods have been applied to predict energy fluctuations in order to create a more dependable and efficient energy system. One machine learning application in that field is forecasting the sun's Global Horizontal Irradiance (GHI). In order to achieve long-term GHI forecasting, this article uses a variety of machine learning techniques, including linear regression and long-short term memory (LSTM) algorithms. Furthermore, the method of predicting the GHI irradiance by using various levels of linear regressors to get the optimal regressor level that offers the lowest error for the testing set based on cross-validation is where this paper's relevance lies. The results demonstrated that the regressor approach offers a lower error for a shorter computational time when compared to a single vanilla LSTM system.

Index Terms—Cross-validation, linear regression, LSTM, renewable energy, Recurrent Neural Network (RNN), Solar irradiance forecasting

INTRODUCTION

Many appeals are being made to produce clean energy, rescue the Earth, and provide mankind a better source of energy in order to protect the environment from the pollution caused by crude oil energy. One way to rescue the planet is via renewable energy. With the world's energy demand growing dramatically and non-renewable energy supplies like coal, natural gas, and crude oil declining, renewable energy sources are becoming more and more important. Furthermore, using non-renewable energy sources results in significant pollution and drastic changes to the climate [1]. Over the last ten years, a large portion of research has concentrated on renewable energy sources, particularly solar and wind energy, as part of attempts to reduce pollution on our planet.

The International Energy Agency (IEA) projects that by 2023, the capacity of renewable energy will have increased by almost 1 Terawatt, or 46% [2]. Like other natural energy sources, solar and wind energy rely on the Global Horizontal Irradiance (GHI) of solar power plants, the wind direction and speed of wind turbines, and other climate phenomena. As a result, the output power varies over time, necessitating calculations to find appropriate power storage units (batteries), determine how to integrate the output power into the network, and determine what control units are required to handle the maximum generated power [3].

Due to the uncertainty around the quantity of GHI and the need for effective energy adaption to the power grid, it is important to compute the GHI over an extended period of time using past data obtained from satellite or ground measurements. Numerous techniques have been developed to forecast solar radiation, and forecasts are also used for solar power plants to identify all potential outcomes that can be utilized to solve the generation and transmission issues. For these reasons, physical, empirical, and statistical methods have been introduced and refined.

The method of predicting the GHI irradiance using various regressor levels to determine the optimal regressor level that offers the lowest error for the testing set reflects the significance of this work. Compared to the LSTM, this regressor approach offers a smaller error for less computing time.

Even though partial linear regression (PLR) is not a novel technique, to the best of our knowledge, we are the first to apply it to long-term solar irradiance prediction. This opens the door to the development of an accurate and simple approach for solar irradiance prediction. Additionally, we tested the prediction step size that yields the best step that satisfies the smallest error for both training and testing using the cross-validation approach.

There are five parts in this study. The regression techniques used to anticipate solar irradiance are presented in Section II. We provide performance analysis, which may be applied to our work, in section III. The applied models and their outcomes are described in Section IV. Section V concludes with a detailed discussion of the findings in relation to future research.

I. Solar Irradiance Forecasting Method

The prediction approaches used for solar irradiance forecasting will be covered in this part, beginning with the most traditional and straightforward methods and progressing to the most modern ones.

A. Physical Model

The physical approaches, which are conventional prediction techniques that are also covered in the literature, were the first efforts to address transmission and generation issues [4-6]. These techniques rely on the PV panel's tilt angle, the sun's angle, the PV's characteristics, and other meteorological factors that affect how much sunlight is absorbed by photovoltaic cells [7]. For the physical approaches to provide correct findings, a lot of data is required. In the literature, other predictor types seem to provide more accurate findings.

B. Empirical Model

One of the most important methods is called the sunshine method. This method is multiple-parameter method that depend on two empirical values: the monthly average of the GHI and the monthly time of sunshine [8]. As shown in Eq. (1)

$$\frac{\text{GHI}}{\text{average}} \quad \frac{S}{a \quad b} \quad H_0 \qquad S_0$$

where S is the monthly average of sunshine, S_0 is the day length, a and b are location empirical values, $GHI_{average}$ is the average global horizontal irradiance predicted monthly, H_0 is the monthly real mean solar radiation [3

C.The Statistical Models

TThe literature focuses increasingly on statistical techniques in order to make more accurate forecasts. In order to forecast future solar irradiance and its absorbable power, these techniques rely on historical GHI values [7]. Machine learning techniques and time-series techniques are two types of statistical techniques.

1) The Time-Series Methods

We can get an indication of future solar irradiation by applying basic calculations and historical data. We are unable to acquire all the circumstances in our mathematical calculations, and these approaches are not particularly precise because of unusual weather variations [9].

Among these techniques, the Auto-Regressive Integrated Moving Average (ARIMA) is one of the most important. These techniques are more precise and versatile than other time series techniques because they are derived from the ARIMA approach, which relies on two components (auto-regression based on the moving average) [10–12].

2) Computational Intelligence

Depending on statistics and to have more accurate results, automated methods have been developed, which

are called computational intelligence, or “Machine Learning (ML) methods.” As we can see from Fig. 1,

where S is the monthly average of sunshine, S_0 is the day length, a and b are location empirical values, $GHI_{average}$ is the average global horizontal irradiance predicted monthly, H_0 is the monthly real mean solar radiation [3].

computational intelligence methods are the second branch of statistical methods. Moreover, they can also be used to improve both the generating and transferring of power from solar energy plants [9].

in solar irradiance prediction [12, 15]. Moreover, multiple linear regression has been surpassed by extreme learning machines (ELM) [16, 17]. A support vector machine (SVM) was created for more precise data, and it uses data mapping to forecast short-term solar irradiance [18].

The researchers looked into more intricate nonlinear techniques since, although producing better findings, it still has limits, especially in long-term prediction. Using all of the factors from previous irradiance levels made this strategy more complicated and challenging to implement for better results (long- and short-term prediction).On the other hand, feed-forward neural networks (FNN) are the simplest approach that resembles the human brain and nervous system. Typically, this kind has three data-processing layers: the input layer, the output

layer, and hidden layers [7, 19, 20]. As an evolution of the FNN, the Recurrent Neural Network (RNN) emerged. To produce fewer errors, the RNN approach uses sequential data with prior states and errors saved internally in iterators [7, 21, 18]. In addition, the Deep Recurrent Neural Network (DRNN), which has several hidden layers, generates more precise results than its counterparts. However, it requires more computing effort than others [7, 22, 23].

There are many types of DRNN, which all have poor long-term memorization traceability when using short-memory connections, and this makes the gradient either explode or disappear. This resulted in the creation of the LSTM approach, which addresses these issues [7, 9, 24], [25]. LSTM is one of the deep learning methods that was designed to avoid long-term dependencies by keeping the information in a separate control unit. It consists of two components: a hidden layer memory cell and a working cell, allowing it to circumvent the gradient exploding (vanishing) issue [26]. The LSTM unit contains three gates instead of two. In addition to the input and output gates, there is also a “forget” gate, which eliminates noise and other unwanted signals from the cell for improved output [16, 26]. Eq. (2) describes the LSTM unit:

$$f_t = g(W_f x_t + U_f h_{t-1} + b_f)\ i_t = g(W_i x_t + U_i h_{t-1} + b_i)$$
$$o_t = g(W_o x_t + U_o h_{t-1} + b_o)\ C_t = f_t c_{t-1} + i_t \check{C}_t)\ h_t = o_t \sigma_t(C_t)$$

outcomes for long-term predictions of the natural phenomenon, some sources used multiple linear regression to overcome the limitations of linear regression to predict long-term states [31], In this paper, it is used multiple linear regression to predict solar radiation for long-term forecasting which is uncommon in previous studies, predicting solar irradiance for short-terms (hours) is very easy by using any machine learning approach, whereas predicting solar for long-term (days, months or year “as done here”), required more efforts [32]. Moreover, the decision to use multiple linear regression for solar irradiance is because the solar irradiance is changing slowly during the day, which makes long-term prediction more important than short-term and mid-term prediction in this field.

II. Performance Analysis

Due to the nonideal nature of the GHI, errors in solar irradiation predictions occur; to eliminate these errors, the system must be analyzed and the faults that have been committed must be examined. One of the following assessment types may be used.

Graphically: predicted data can be compared with measured data so we can visually recognize errors and differences. Many kinds of literature use time series plots, scatter plots, or Receiver Operating Characteristic (ROC) curves [15].

Statistically: the graphical “traditional” methods are

$$\check{C} = (W x + U h + b) \quad (2)$$

not enough to test the results. More accurate and more

$$t \quad g \quad c \quad t \quad c \quad t \square 1 \qquad c$$
$$C_t \square f_t c_t \square 1 \square i_t \check{C}_t) h_t \square o_t \square_t (C_t)$$

where f_t is the forget gate; i_t is the input gate; O_t is the output of h_t, which is the output of the hidden gate; $h_{t\square 1}$ is the hidden state output of the previous LSTM block; C_t represents the cell state; $\check{C}_t$ represents the candidates for cell state at timestamp t; $\square$ is the sigmoid function; x_t is the input of the current timestamp. W_f, W_i, W_o, W_c, U_f, U_i, U_o, and U_c are the weights of the respective gates, and b_f, b_i, b_o, and b_c are the biases for the respective gates. Weights and bases remain constant throughout all steps and do not change from one time step to the next [27-30], LSTM neural network architecture is shown in Fig. 2.

detailed results are needed. The statistical method can give us what we need. Many statistical formulas are used for our objectives. The most commonly used method is, the root mean square error (RMSE), which is also used for analyzing the systems. RMSE can be calculated using Eq. (3):

RMSE $\square$

$$\sqrt{\frac{1}{M}\sum_{i=1}^{M}(y_i - \hat{y}_i)^2} \quad (3)$$

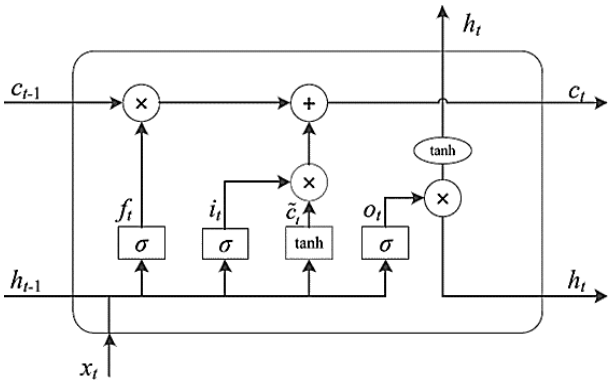


Fig. 2. LSTM structure network.

Rather of using this intricate approach, and by going back to linear regression, which has the primary drawback of bad

Description of the database: In addition to the date, rainfall, snowfall, wind direction, and other information, the database used in this study includes a number of weather-related details. The Modern-Era Retrospective Analysis for Research and Applications, Version 2 (MERRA-2), which is being constructed as a "milestone" for next integrated Earth system analyses (IESAs), is the source of this database. The database comprises data from 1490 days with solar irradiance recorded every 24 hours at the time of maximum daily irradiance; these 1490 records are separated into the training set and testing set [33]. MERRA-2 has many quality improvements and decreases in erroneous trends and system-related faults. While wind speed is measured at a distance of 10 m, this type of technology provides GHI, rainfall, and snowfall probabilities along with temperature, relative humidity, and pressure at a distance of 2 m from the land [34–36]. The data from this technology is widely used in literature and for numerous fields. The dataset covers a point at latitude 36,356 (positive indicates north) and longitude 43,125 (positive means east) in Mosul, Iraq, between December 1, 2016, and December 31, 2020.

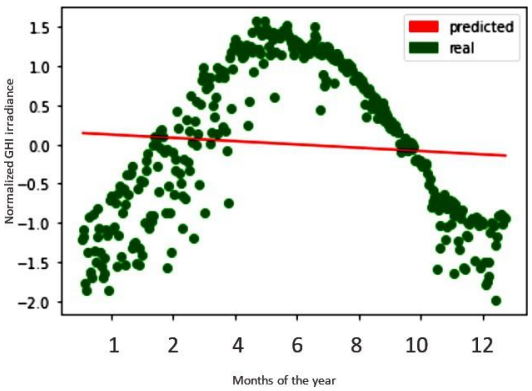
Only the days of the year are used in this research to estimate solar irradiance, which is more significant for us since irradiance changes slowly during the day and other factors like wind speed and rainfall are now disregarded.

III. Models Implementation

Python programming was used to evaluate the MERRA-2 and provide one-year projections. The LSTM model is the fifth of the five deployed models; the other four depend on linear prediction. Two years of training data and one year of testing data are separated out for each model. The outliers have no bearing on the outcomes since they are set to the average.

A. Linear Predictors

Initially, a single predictor is used for the entire year. In the second model, the year is divided into four parts for which four predictors are applied. The third model divides the year into 12 parts. The fourth model divides the year into twenty-four parts. The following formula clearly demonstrates linear prediction.



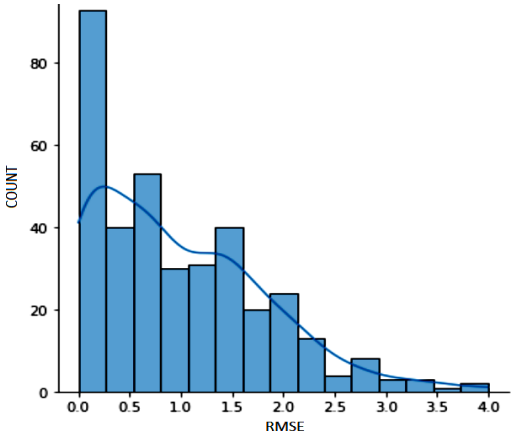


Fig. 3. One-part regression (whole year) output.

$$Y_i = \beta X_i + e_i \quad (4)$$

where Y_i is dependent variable (to be predicted), X_i is the independent variable (to be used in Y prediction), β is the Regression coefficient, e_i is the error.

IV. Results and Discussion

The forecasting results will span five-time frames: one-year, seasonal forecasting (four months), monthly forecasting, half-month forecasting, and weekly forecasting. Accordingly, each of these scenarios will involve a number of regressors.

$X_1 \quad e_1$
$X \quad e$

Fig. 4. RMSE for one-part regressor

B. Season Forecasting (Four Regressors)

Due to the inaccuracy of the (one regressor) model, the year has been divided into four parts, each part represents a distinct season. Using the same equation for each regressor, the outcome of our design is shown in Fig. 5.

The output curve shows that the model performs better than a single regressor model. The average of each season

i

X_n e_n

Every equation is used to predict a specific period of time, in another word there are many simple linear models that work together to form the final prediction curve. Later, we will compare the results with the LSTM results.

A. Whole Year Forecasting (One Regressor)

Short-term results from the single-regressor model are acceptable, but as can be seen in Fig. 3, over longer time periods, the model introduces extremely bad results.

The RMSE is depicted in Fig. 4 and demonstrates that the result differs significantly from the actual data (it gives the mean irradiance for the entire year). It is obvious that the system produces results with high errors (most days have an RMSE of 1 up to 4). Fig. 4 depicts the distribution of points along the range of RMSE, where around 90 points may have an RMSE equal to 0.3. As RMSE increases, we observe that the number of points decreases.

to the low probability of cloud formulation. The probability distribution of the RMSE of the model is depicted in Fig. 6. It indicates that more points are located closer to the left, resulting in a lower RMSE, which is preferable to the RMSE for a one-part regressor. Evidently, error levels have decreased since the majority of errors are smaller than 2.

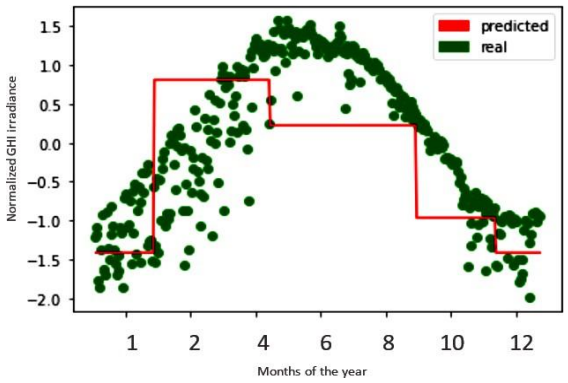
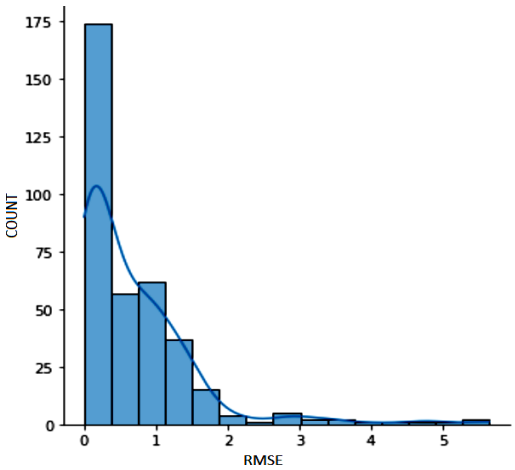


Fig. 5. Four regressors output.



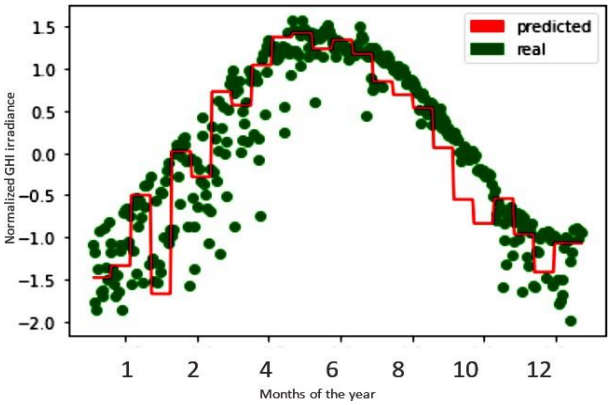


Fig. 6. RMSE for four regressors.

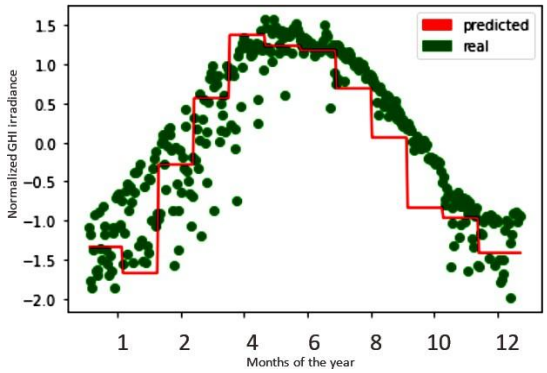


Fig. 7. Twelve regressors output.

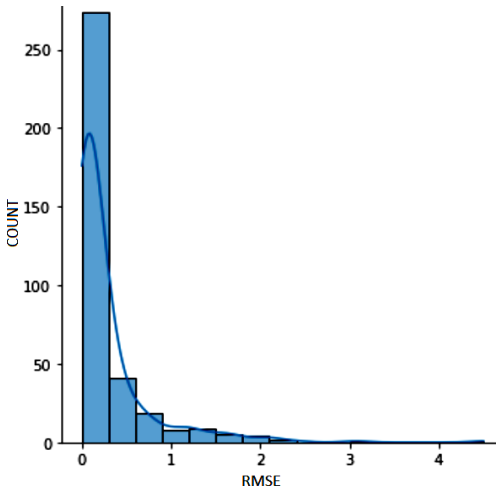


Fig. 8. RMSE for twelve regressors.

C. Monthly Forecasting (Twelve Regressors)

Although the RMSE for four regressors is less than 2 units, a more precise result is required. As illustrated in Fig. 7, this model uses a predictor for each month to achieve better results.

Based on Fig. 7, the predicted irradiance is closer to the actual data, and we can observe the RMSE probability distribution to examine our results in further depth.

According to the graph in Fig. 8, the number of days with errors of three or four units approaches zero, while the number of days with errors of less than half a unit increases (more than 250 days have that RMSE).

Fig. 9. Twenty-four-part regressors output

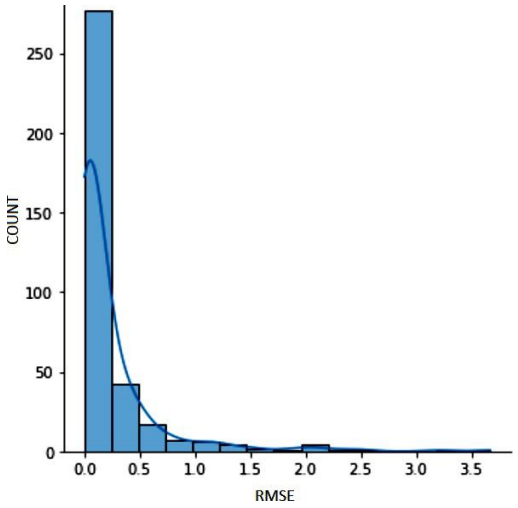


Fig. 10. RMSE for twenty-four regressors.

D. Half-Month Forecasting (Twenty-Four Regressors)

To improve the precision of the results, more regressors are added, one for every 15 days, as seen in Fig. 9. While Fig. 10 displays the RMSE probability distribution.

E. Weekly E-Budget (Fifty-Two Regressors)

For more precise predictions, fifty-two linear regressors are used separately. Fig. 11 depicts the forecasts. And the RMSE probability distribution is shown in Fig. 12.

Because there was no discernible difference in the RMSE curves between the (24-regressors and 52-regressors) scenarios, no more regressors were introduced.

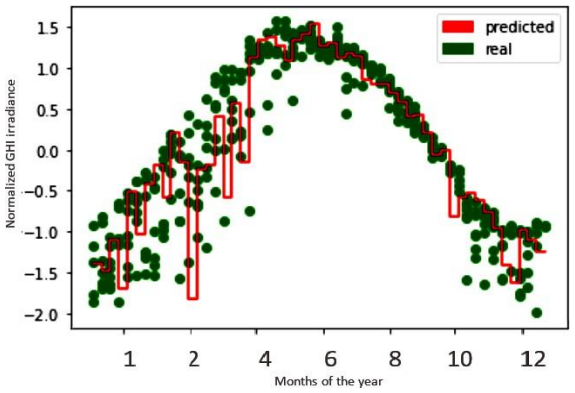


Fig. 11. Fifty-two-part regressors output.

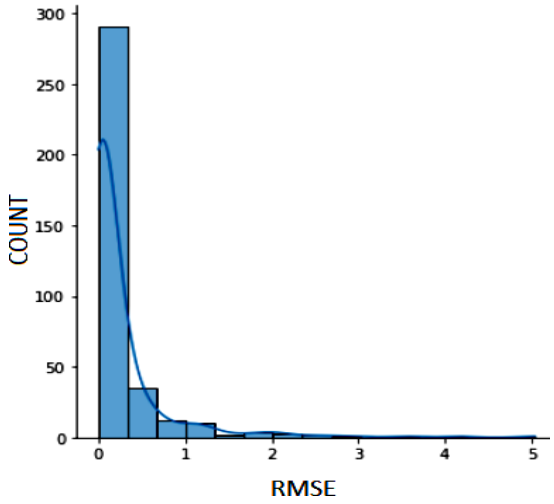


Fig. 12. RMSE for fifty-two-part regressors.

F. Cross-Validation

Increasing the number of regressors improves training performance since training and testing data are kept apart. The testing phase follows suit, adding more regressors to the testing set as a result of "overfitting" for training that may not be appropriate for testing. Table I provides the RMSE for both training and testing. We can see that the training error falls as the number of regressors rises. However, up to the twenty-fourth regressor, the error in the testing set reduces; beyond that, the RMSE of the testing set rises.

The fourth column of Table I displays the Min-RMSE, which represents the smallest RMSE shared across training and testing—the objective of cross-validation. Referring to Fig. 9 in comparison to Figs. 3, 5, 7, and 9, it is clear that the minimum RMSE value we achieved in the Table is at twenty-four linear predictors.

TABLE I: THE CROSS-VALIDATION OF TESTING AND TRAINING

Method	RMSE in training	RMSE in testing	Min-RMSE training/ testing
One linear predictor	0.984	0.9799	
Four linear predictors	0.456	0.4611	
Twelve linear predictors	0.261	0.2812	
Twenty-four linear predictors	0.221	0.2277	0.221/ 0.2277
Fifty-two linear predictors	0.212	0.2475	
One hundred and four linear predictors	0.211	0.4382	

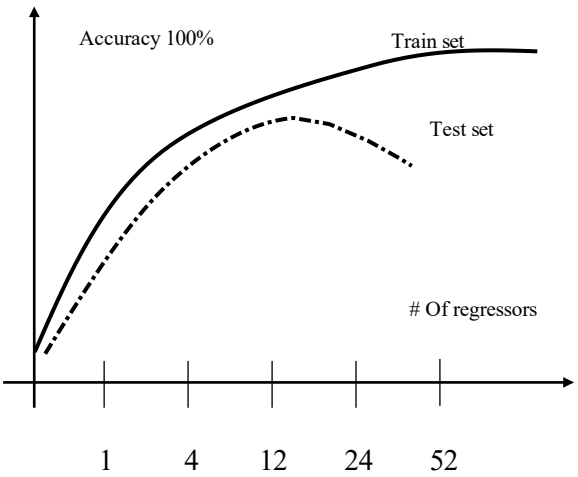


Fig. 13. The cross-validation of the training and testing.

The accuracy as a function of the number of regressors for the training set and testing set is depicted in Fig. 13. A number of regressors boost the accuracy of the training set. Nonetheless, the testing set improves accuracy. After the twenty-four regressor, the problem of overfitting occurs in the linear predictor. Consequently, the twenty-fourth regressor is the optimal regressor level for predicting the weather based on training data.

G. LSTM Predictor

With only one hidden layer and one output, the vanilla LSTM is the most basic LSTM model. There are 24 input units, one every fifteen days. The first layer processes the inputs, which are then sent to the hidden layer and the output layer, which provides the forecasts for the chosen time frame of the year. Because the data is separated in this model, 32 samples are analyzed simultaneously each time. Stated otherwise, 32 is the selected batch size. Although it will take too long, selecting a number lower than 32 could provide better results. 100 is chosen as the epoch. In order to get better results, the model will thus iterate up to 100 times for each batch. Because of its superior efficiency and quick convergence over other optimizers, the Augmented Dynamic Adaptive Model (ADAM) optimization model in Python is used as an optimizer. The LSTM prediction results for the specified model are shown in Fig. 14.

It is evident that the LSTM model can anticipate the full year with a pure curve that is not overfitted. The RMSE is shown in Fig. 15 below.Most of the time, the error in the forecasts is less than 0.6, which is a desirable number, making LSTM one of the most accurate methods.

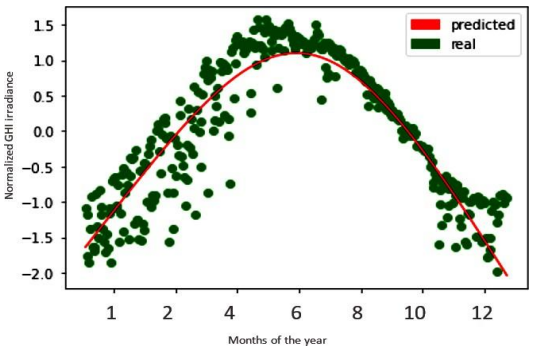


Fig. 14. LSTM output

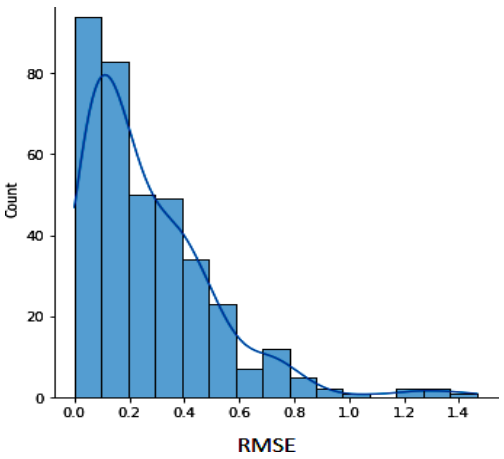


Fig. 15. RMSE for LSTM output

H. Discussion

The RMSE and processing time for each model are summarized in Table II.

TABLE II: RMSE AND PROCESSING TIME FOR DIFFERENT MODELS

Method	RMSE in average	Processing time
One linear predictor	0.9799	0.4264 second
Four linear predictors	0.4611	0.4308 second
Twelve linear predictors	0.2812	0.4329 second
Twenty-four linear predictors	0.2277	0.6397 second
Fifty-two linear predictors	0.2475	2.739 seconds
Vanilla LSTM	0.360	6.8090 second

Table II shows that there are several methods to utilize linear regression to get results that are close to the real values and to vanilla LSTM, where the error of the single linear regressor is large all year long (providing an average value for the year). The time needed to finish the prediction rises with the number of regressors, and the RMSE value falls. When twelve regressors are added to the model, the RMSE decline gets smaller; twelve and twenty-four regressors provide superior results. Nevertheless, greater outcomes are not always achieved by increasing the number of regressors. For a longer period of time, the fifty-two regressors provide less accurate findings. Additionally, this outcome supports Table I's cross-validation result, which shows that the twenty-four linear predictors perform the best in terms of accuracy.

In contrast, the RMSE of the LSTM model is worse than that of twelve and twenty-four regressors, and it produces pure curvilinear outcomes and takes a very long time to attain conclusions. The 24-regressor model took 0.64 seconds and had an RMSE of 0.227, whereas the LSTM took 6.8 seconds and had an RMSE of 0.36. The twenty-four linear model outperforms the LSTM model as a consequence of these findings. The fundamental principle of the system is supported by the comparison of the results figures and RMSE values, which show that the projected values are more closely matched with the actual irradiance levels.

CONCLUSION

Forecasting the whole long term with a single regressor may not provide the same results as breaking the long term down into smaller periods and utilizing the simplest methods. The findings will be non-curvilinear due to the non-ideality of natural occurrences. More precise data will show up as the number of linear regressors increases. Despite having a non-over-fitted curve, the LSTM has complex parameters that must be selected by experimenting with various values until the model performs better. In addition to processing time, that requires extra time. Because of this, more work may be required in the future to improve forecasts and have an output shape that is closer to the curve.

REFERENCES

[1]K. Yan, H. Shen, L. Wang, H. Zhou, M. Xu, and Y. Mo, "Hybrid deep learning-based short-term solar irradiance forecasting," Information, vol. 11, no. 1, Jan. 2020, doi: 10.3390/info11010032.

[2] M. Gao, J. Li, F. Hong, and D. Long, "Day-ahead power forecasting in a large-scale photovoltaic plant based on weather classification using LSTM." Energy, vol. 187, #115838, Nov. 2019.

[3]E. Quansah, L. K. Amekudzi, K. Preko, J. Aryee, O. R. Boakye, D. Boli, and M. R. Salifu, "Empirical models for estimating global solar radiation over the Ashanti Region of Ghana," Journal of Solar Energy, vol. 2014, pp. 1–6, January 2014.

[4]M. U. Siddiqui, O. K. Siddiqui, A. B. S. Alquaity, H. Ali, A. F. M. Arif, and S. M. Zubair, "A thorough analysis of multi-physics modeling of solar modules," Energy Conversion and Management, vol. 258, #115414, April 2022.

[5] A. Dolara, S. Leva, and G. Manzolini, "Comparison of different physical models for PV power output prediction," Solar Energy, vol. 119, pp. 83–99, Sep. 2015, doi: 10.1016/j.solener.2015.06.017 [6] IEA (2018), Renewables 2018, IEA, Paris https://www.iea.org/reports/renewables-2017 [7] Alzahrani, P. Shamsi, C. Dagli, and M. Ferdowsi, "Solar irradiance forecasting using deep neural networks," Procedia Computer Science, vol. 114, pp. 304–313, 2017.
[8] S. Shamshirband, T. Rabczuk, and K. W. Chau, "A survey of deep learning techniques: application in wind and solar energy resources," IEEE Access, vol. 7, pp. 164650–164666, 2019.
[9] "Proposal of a regressive model for the hourly diffuse solar radiation under all sky conditions," Energy Conversion and Management, vol. 51, no. 5, pp. 881–893, May 2010, J. A. Ruiz-Arias, H. Alsamamra, J. Tovar-Pescador, and D. Pozo-Vázquez.
[10] S. Siami-Namini, N. Tavakoli, and A. Siami Namin, "A comparison of ARIMA and LSTM in forecasting time series," Proceedings of the 17th IEEE International Conference on Machine Learning and Applications, December 2018. doi: 10.1109/ICMLA.2018.00227.
[11] "Machine learning methods for solar radiation forecasting: A review," Renewable Energy, vol. 105, pp. 569–582, 2017; C. Voyant, G. Notton, S. Kalogirou, M. L. Nivet, C. Paoli, F. Motte, and A. Fouilloy. 10.1016/j.renene.2016.12.095 is the doi.
[12] "The modern-era retrospective analysis for research and applications, Version 2 (MERRA-2)," Journal of Climate, vol. 30, no. 14, pp. 5419–5454, July 2017; R. Gelaro, W. McCarty, M. J. Suárez, et al.
[13] Short-term load forecasting using multiple linear regression for huge data, A. Y. Saber and A. K. M. R. Alam, Proceedings of the IEEE Symposium Series on Computational Intelligence (SSCI), November 2017, doi: 10.1109/ssci.2017.8285261.
[14] K. Hirose, "Interpretable modeling for short- and medium-term electricity demand forecasting," Frontiers in Energy Research, vol. 9, Dec. 2021, doi: 10.3389/fenrg.2021.724780.
[15] T. Lehtola and A. Zahedi, "Technical challenges in the application of renewable energy: A review," International Journal of Smart Grid and Clean Energy, pp. 689–699, 2020, doi: 10.12720/sgce.9.3.689-699
[16] H. Suyono, H. Santoso, R. Nur Hasanah, U. Wibawa, and I. Musirin, "Prediction of solar radiation intensity using extreme learning machine," Indonesian Journal of Electrical Engineering and Computer Science, vol. 12, no. 2, Nov. 2018, doi: 10.11591/ijeecs.v12.i2.pp691-698.
[17] M. Abdillah, W. Pramudito, T. Nugroho, and D. Fitria, "Solar irradiance forecasting using kernel extreme learning machine: Case study at Lamongan and Muara Karang Regions, Indonesia," Journal of Engineering Science and Technology, vol. 17, no. 2, pp. 1561-1576, 2022.
[18]M. Z. Hassan, M. E. K. Ali, A. B. M. S. Ali, and J. Kumar, "Day-ahead solar radiation forecasting using machine learning approach," Proceedings of the 4th Asia-Pacific World Congress on Computer Science and Engineering (APWC on CSE), December 2017. 10.1109/APWConCSE.2017.00050 is the doi.
[19] Y. LeCun, Y. Bengio, and G. Hinton, "Deep learning," Nature, vol. 521, no. 7553, pp. 436–444, 2015, doi: 10.1038/nature14539.
[20]Learning and verification of feedback control systems using feedforward neural networks, S. Dutta, S. Jha, S. Sankaranarayanan, and A. Tiwari, IFAC-Papers on Line, vol. 51, no. 16, pp. 151–156, 2018, doi: 10.1016/j.ifacol.2018.08.026.
[21]Deep learning for time series forecasting: The electric load scenario, A. Gasparin, S. Lukovic, and C. Alippi, CAAI Trans. on Intelligence Technology, vol. 7, no. 1, pp. 1–25, Sep. 2021. 10.1049/cit2.12060.
[22] J. Cao and X. Lin, "Hourly and daily solar irradiation forecast using diagonal recurrent wavelet neural networks," Energy Conversion and Management, vol. 49, no. 6, pp. 1396–1406, June 2008.
[23] T. Ozdemir, F. Taher, B. O. Ayinde, J. M. Zurada, and O. Tuzun Ozmen, "Comparison of feedforward perceptron network with LSTM for solar cell radiation prediction," Applied Sciences, vol. 12, no. 9, #4463, April 2022, doi: 10.3390/app12094463.
[24] G. Reikard, "A comparison of time series forecasts for solar radiation prediction at high resolutions," Solar Energy, vol. 83, no. 3, pp. 342–349, March 2009.
[25]M. Diagne, M. David, P. Lauret, J. Boland, and N. Schmutz, "A proposal for small-scale insular grids and a review of solar irradiance forecasting methods," Renewable and Sustainable Energy Reviews, vol. 27, pp. 65–76, Nov. 2013, doi: 10.1016/j.rser.2013.06.042.
[26]A. Milad, I. Adwan, S. A. Majeed, N. I. M. Yusoff, N. Al-Ansari, and Z. M. Yaseen, "Emerging technologies of deep learning models development for pavement temperature prediction," IEEE Access, vol. 9, pp. 23840–23849, 2021.
[27] P. Anki and A. Bustamam, "Measuring the accuracy of LSTM and BiLSTM models in the application of artificial intelligence by applying chatbot program," Indonesian Journal of Electrical Engineering and

Computer Science, vol. 23, no. 1, July 2021, doi: 10.11591/ijeecs.v23.i1.pp197-205.
[28] Y. Yu, J. Cao, and J. Zhu, "An LSTM Short-Term Solar Irradiance Forecasting Under Complex Weather Conditions," IEEE Access, vol. 7, pp. 145651–145666, 2019.
[29] J. Schmidhuber and S. Hochreiter. "Long-term short-term memory" Neural Computation, Volume 9, Issue 8, November 1997, pp. 1735–1780.
[30] P. P. Phyo, C. Jeenanunta, and K. Hashimoto, "Deep learning models for electricity load forecasting in Thailand," International Journal of Electrical and Electronic Engineering & Telecommunications, vol. 8, no. 4, pp. 221–225, 2019.
[31] W. González-Manteiga, M. Febrero-Bande, and M. Piñeiro-Lamas, "Semiparametric prediction models for variables related with energy production," Journal of Mathematics in Industry, vol. 8, no. 1, August 2018, doi: 10.1186/s13362-018-0049-0.
[32] "Dynamic forecasting of solar energy microgrid systems using feature engineering," IEEE Trans. on Industry Applications, vol. 58, no. 6, pp. 7857-7869, Nov.-Dec. 2022, M. Mohamed, F. E. Mahmood, M. A. Abd, A. Chandra, and B. Singh.
[33] MERRA-2, or Modern-Era Retrospective Analysis for Research and Applications, Version 2. [34] https://gmao.gsfc.nasa.gov/reanalysis/MERRA-2/
S. B. Shams, V. P. Walden, J. W. Hannigan, W. J. Randel, I. V. Petropavlovskikh, A. H. Butler, and A. de la Cámara, "Using MERRA-2 to analyze ozone variations and uncertainties at high latitudes during sudden stratospheric warming events," Atmospheric Chemistry and Physics, vol. 22, no. 8, pp. 5435–5458, April 2022.
[35] Massive-parallel trajectory calculations version 2.2 (MPTRAC-2.2): Lagrangian transport simulations on graphics processing units (GPUs)," Geoscientific Model Development, vol. 15, no. 7, pp. 2731–2762, Apr. 2022; [36] L. Shikwambana, "Global distribution of clouds over six years: A review using multiple sensors and reanalysis data," Atmosphere, vol. 13, no. 9, Sep. 2022, doi: 10.3390/atmos13091514.